J. Phys. B: At. Mol. Opt. Phys. 24 (1991) 4231-4244. Printed in the UK

State-selective double capture in collisions of bare ions with helium atoms at low energies: II. Ejected-electron spectra

Z Chen and C D Lin

Department of Physics, Kansas State University, Manhattan, KS 66506, USA

Received 14 October 1990, in final form 17 April 1991

Abstract. The Auger electron spectra of doubly excited states of ions resulting from double capture in collisions of bare ions with helium atoms in the energy range of a few keV amu^{-1} are calculated. The electron capture amplitudes are obtained in the independent-electron approximation. By combining these amplitudes with the Auger decay amplitudes and taking into account the post-collision interaction effect and the interference from different states, the electron spectra as a function of the ejection angles are evaluated. Calculations have been carried out for the electron spectra of $2l3l'$ doubly excited states of C^{4+} from C^{6+}-He collisions and of $3l3l'$ doubly excited states of O^{6+} from O^{8+}-He collisions. The theoretical results are compared with measured Auger electron spectra.

1. Introduction

In recent years, high-precision projectile Auger electron spectroscopy has been used in many laboratories to measure the electron spectra from the autoionization of doubly excited states of projectiles following double electron capture (Bordenave-Montesquieu *et al* 1988, Mack *et al* 1989, Stolterfoht *et al* 1990, Moretto-Capelle *et al* 1989, Posthumus and Morgenstern, 1990, Holt *et al* 1991, Boudjema *et al* 1991) or transfer excitation processes in collisions of multiply charged ions with atoms and molecules. The electron spectra are often measured at one or a few angles from which experimentalists deduced the absolute or the relative cross sections for the formation of individual doubly excited states. To get such information, however, a number of assumptions about the formation and the decay of doubly excited states must be made. Some of these assumptions are not justified and the deduced 'experimental' cross sections must be treated with care.

In the previous paper (Chen *et al* 1991), we calculated the cross sections for double capture to individual doubly excited states based on an independent-electron approximation. In this article, we calculate the theoretical angular dependence of the emitted electron spectra to compare with experimental Auger electron spectra. For ion-atom collisions where the projectile incident energy is of the order of a few keV amu^{-1} or greater, the collision time is short compared with the decay time of the doubly excited states. Thus the ejected-electron spectra can be considered to be formed in a two-step process where doubly excited states are first collisionally populated, followed by Auger emissions. In this article we discuss the angular distribution of the emitted electrons.

The angular distribution of the Auger electron of an isolated excited state has been studied over the years (Cleff and Mehlhorn 1974, Aberg and Howat 1982). For the doubly excited states populated by ion-atom collisions two other effects must be

0953-4075/91/194231+14$03.50

considered. First, the Auger emission occurs in the electric field of a receding ion such that the angular distribution is different from that of an isolated atom or ion. This has been called the post-collision interaction (PCI) effect in general. Second, the Auger widths of some doubly excited states are comparable to the energy separations between neighbouring states such that the Auger emission from different states must be treated coherently. Since each doubly excited state can also decay radiatively, the branching ratio for the Auger emission of each state must be taken into account as well.

The theoretical model used for the calculation of the electron spectra is given in section 2. In section 3, the model is applied to analyse the electron spectra of $2l3l'$ doubly excited states of C^{4+} resulting from the collision of C^{6+} on He and of $3l3l'$ doubly excited states of O^{6+} resulting from the collision of O^{8+} on He. The angular distributions of the electron spectra are analysed and the results compared with the experimental data. The conclusions are given in section 4.

2. The theoretical model

As described in the introduction, for the collisions studied here the Auger emission can be considered as a two-step process where individual doubly excited states are formed in the capture process, followed by autoionizations. To calculate the electron's spectra, several factors must be considered: (1) each doubly excited state populated is aligned in general, i.e., the cross section for each magnetic substate is not equal. This would result in anisotropic angular distributions; (2) each state has a non-zero fluorescence yield which must be considered; (3) the ejected-electron's spectrum for each state is modified by the PCI effect. This effect changes the electron's spectra from the symmetric Lorentzian shape to an asymmetric shape stretching toward the lower energy side; (4) when doubly excited states are not well separated, the ejected-electron spectra from neighbouring states must be added coherently.

2.1. *The angular distribution of Auger electrons from an isolated doubly excited state*

We choose the quantization axis to be along the direction of the incident projectile. An electron ejected in the direction $\boldsymbol{k}$ is described by

$$|\boldsymbol{k}\rangle = \frac{4\pi}{kr} \sum_{l=0}^{\infty} \sum_{m=-l}^{l} \mathrm{i}^l \, \mathrm{e}^{\mathrm{i}\sigma_l} F_l(kr) \, Y^*_{lm}(\hat{\boldsymbol{k}}) \, Y_{lm}(\hat{r}) \tag{1}$$

where σ_l is the phaseshift, $F_l(kr)$ the radial wavefunction of the electron and Y_{lm} the spherical harmonics, with $\hat{\boldsymbol{k}}$ in the direction of propagation and $\hat{r}$ the spherical angles of the electron. The Auger decay of each doubly excited state is described by the matrix element

$$T_{if}(\alpha LM \to nl_1 \varepsilon l_2, \boldsymbol{k}) = \langle \alpha LM | V_{\mathrm{A}} | nl_1 \varepsilon l_2 LM \rangle \sum_{m_1 m_2} \langle l_1 l_2 m_1 m_2 | LM \rangle \, Y^*_{l_2 m_2}(\boldsymbol{k}) \tag{2}$$

where the initial doubly excited state is described by $|\alpha LM\rangle$. The final state after the Auger emission is given by $|nl_1 \varepsilon l_2 LM\rangle$, where $|nl_1\rangle$ is the one-electron state of the ion and l_2 is the angular momentum of the Auger electron with energy $\varepsilon = k^2/2$. The operator V_{A} is the electron–electron Coulomb interaction. The initial-state wavefunction $|\alpha LM\rangle$ is calculated by the configuration interaction (CI method, where α stands for the other quantum numbers ${}_n(K, T)^{\mathrm{A}}_N$ used to designate each doubly excited state

(Lin 1986). Note that we do not use the independent-electron quantum numbers to describe doubly excited states.

The angular dependence for detecting an electron at angle $k=(\theta, \phi)$ with respect to the incident direction from an isolated initial state $|\alpha L\rangle$ is given by

$$I(\boldsymbol{k}) = 2\pi |T_{if}(\alpha L \to \boldsymbol{k})|^2$$

$$= 2\pi \sum_{nl_1} \sum_{M} \left| a_{LM}(\theta_p) 4\pi \sum_{l_2} e^{i(\sigma_{l_2} + l_2 \pi/2)} \right.$$

$$\left. \times \langle \alpha LM | V_A | nl_1 \varepsilon_k l_2 LM \rangle \sum_{m_1 m_2} \langle l_1 l_2 m_1 m_2 | LM \rangle Y^*_{l_2 m_2}(\boldsymbol{k}) \right|^2 . \tag{3}$$

The probability amplitude for populating the initial state $|\alpha LM\rangle$ by the primary collision is given by $a_{LM}(\theta_p)$ where θ_p is the scattering angle of the projectile. For collisions where the projectile scattering angles are not measured, the ejected-electron spectra is obtained by integrating over θ_p. In such integral measurements, the electron spectra do not depend on the azimuthal angle ϕ. The angular dependence on θ can be obtained by averaging over ϕ using

$$\int Y^*_{l_2 m_2}(\boldsymbol{k})\, Y_{l_2' m_2'}(\boldsymbol{k})\, d\phi$$

$$= \tfrac{1}{2}(-1)^{m_2} \delta_{m_2 m_2'} \sum_{J} (2J+1)[(2l_2+1)(2l_2'+1)]^{1/2}$$

$$\times \begin{pmatrix} l_2' & l_2 & J \\ 0 & 0 & 0 \end{pmatrix} \begin{pmatrix} l_2' & l_2 & J \\ m_2' & -m_2 & 0 \end{pmatrix} P_J(\cos\theta) \tag{4}$$

where the bracket denotes the 3-j symbols. The general expression in (3) for each $|nl_1\rangle$ state of the ion can be rewritten in the form

$$I(\theta) = \sum_{l} A_l P_l(\cos\theta) \tag{5}$$

where l is limited to even integers, and A_l is related to the alignment parameters. This simple situation occurs, for example, in the decay of $2l3l'$ doubly excited states to the $1s\varepsilon l''$ continuum. If the initial state has total angular momentum L, this requires that $l_2 = L$ since $l_1 = 0$, see equation (3). Thus the angular distribution for each M-component is given by $|Y_{LM}(\theta, \phi)|^2$ and the ejected-electron spectra are symmetric with respect to $\theta = 90°$ in the emitter frame. Deviation from the symmetric distribution occurs: (i) when the continuum state can be populated also by direct processes leading to the $1s\varepsilon l''$ continuum, (ii) when the PCI effect is large, and (iii) when the state cannot be treated as an isolated state, i.e., when the width of the state under consideration is not small compared with the energy separation between neighbouring states. The effect in (i) above is well known and it leads to typical asymmetric Fano resonance profiles in the electron spectra. Since the direct process leading to the $1s\varepsilon l''$ continuum is a transfer ionization process and is important only at much higher collision energies, it can be neglected for the present low-energy collisions.

2.2. The PCI effect and the interference of autoionizing transitions

For the low energy collisions considered here, the PCI effect and the effect due to the overlapping resonances are more important. The PCI effect is a three-body phenomenon and there exists no exact treatment. For the present collision systems, doubly excited states of the projectile autoionize in the receding field of the recoil ion, He^{2+}. There

are a number of theoretical models in the literature (Barker and Berry, 1966, Devdariani *et al* 1977, Morgenstern *et al* 1977, Niehaus 1977, Arcuni 1986, van der Straten and Morgenstern 1986a, b, van der Straten *et al* 1988, Barrachina and Macek 1989) for treating such PCI effects. We follow the model of van der Straten and Morgenstern (1986a, b) for each isolated state, and the coherence in the electron emission is obtained by summing over the Auger emission amplitudes from all the states (Mack *et al* 1989). The intensity of the electron's spectra is then given by

$$I(k)=2\pi\sum_{nl_1}\sum_{M}\left|\sum_{\alpha}f^{\alpha}(\varepsilon,\varepsilon_L)a^{\alpha}_{LM}(\theta_p)4\pi\sum_{l_2}e^{i(\sigma_{l_2}+l_2\pi/2)}\right.$$
$$\left.\times\langle\alpha LM|V_A|nl_1\varepsilon_k l_2 LM\rangle\sum_{m_1m_2}\langle l_1l_2m_1m_2|LM\rangle Y^*_{l_2m_2}(\boldsymbol{k})\right|^2 \tag{6}$$

which is a straightforward generalization of (3). In (6), the amplitudes for autoionization from each doubly excited state to the same final $|nl_1\rangle$ state of the ion are added coherently. The PCI effect for each state is represented by a lineshape function $f^{\alpha}(\varepsilon,\varepsilon_L)$. If there is no PCI effect, this function gives the Lorentzian shape for each state. In this work we use the lineshape function of van der Straten and Morgenstern (1986a)

$$|f(\varepsilon,\varepsilon_L)|=\left(\frac{2q}{v\Gamma_r(1+\varepsilon_r^2)\sinh(\pi q/v)}\right)^{1/2}\exp\left(\frac{\pi q}{2v}\left[1+\frac{2}{\pi}\tan^{-1}(-1/\varepsilon_r)\right]\right)$$
$$\arg(f)=-\frac{q}{v}\left(\ln(\Gamma_r/2)+\frac{1}{2}\ln(1+\varepsilon_r^2)\right)-\tan^{-1}(-1/\varepsilon_r)-\pi/2-\arg(\Gamma(1+iq/v)) \tag{7}$$

where Γ_r is the natural width, $\varepsilon_r=2(\varepsilon-\varepsilon_L)/\Gamma_r$, $q=Q(1-v/|v-v_0|)$, Q the charge of the PCI inducer, v the velocity of the projectile and v_0 the velocity of the emitted electron in the emitter frame.

The PCI formula given above has been shown to work quite well in describing the PCI effects for collisions at higher energies (van den Brink *et al* 1989). The PCI effect shifts the position of the resonance energy and changes the lineshape from a Lorentzian to one which tends to skew toward lower electron velocity. In equation (7) we note that the Stark effect of the neighbouring resonances has not been included despite the fact that several models have been proposed (Stolterfoht *et al* 1979, Miraglia and Macek 1990).

Equation (6) clearly shows that it is difficult to deduce double capture cross sections of individual doubly excited states from the measured electron spectra at a given angle $\boldsymbol{k}$ for integral measurements where (6) has been integrated over the scattering angles θ_p of the projectile. Even if one assumes that electrons originating from different doubly excited states do not interfere, in general one still needs to know the phases of the Auger matrix elements and the scattering phaseshifts. Simple situations occur when the final one-electron ion after the Auger process is a 1s state. In this case, the phases mentioned above do not enter. We will discuss this further in the following.

3. Results and discussion

3.1. Angular distributions of an isolated doubly excited state

The angular distribution for the Auger electron from each isolated state is given by equation (3). In the special case that the ion is left in the 1s state ($n=1$ and $l_1=0$),

there is only one term in the summation over l_2, $l_2 = L$. The angular distribution for each magnetic substate $|\alpha LM\rangle$ is then given by $|Y_{LM}(\theta, \phi)|^2$. Since the function $|Y_{LM}(\theta, \phi)|^2$ vanishes at $\theta = 0°$ if $M \neq 0$, observation of Auger electrons at 0° only measures the cross section for populating the $M = 0$ component of the excited state. This general result is correct for the (2, 2) and (2, 3) doubly excited states of two-electron ions.

The angular distribution for each of the doubly excited states in the (3, 3) manifold is much more complicated since each state can decay to 1s, 2s and 2p states of the ion. The branching ratio for the decay to 1s is negligible and will not be discussed further. For the decay to 2s and 2p states the resulting Auger electrons have identical energies but there is no interference in the electron spectra from these two channels since the final states of the ion after the Auger emission have different angular momenta (Morgenstern *et al* 1990). For the decay to 2p states, the summation over l_2 ($l_2 = L-1$ and $L+1$) must be carried out coherently and the scattering phaseshifts and the phases in the Auger matrix elements are needed. On the other hand, the resulting Auger angular distribution for each M-component of the initial state $|\alpha LM\rangle$ is still given by (5), i.e., the angular distribution for each M-component remains symmetric with respect to $\theta = 90°$, since the two Y_{lm} functions which are added coherently are either both even or both odd functions. In this case, the electron intensity measured at 0° includes not only the $M = 0$ component but also the $M \neq 0$ components of the initial state $|\alpha LM\rangle$. To fit measured electron spectra, it is obvious that a number of fitting parameters are needed.

The calculated angular distributions for each M-component of an isolated doubly excited state in the (3, 3) manifold of O^{6+} are given in figure 1 where each state is labelled by the K and T quantum numbers, in addition to the usual L, S and π. Since $A = +1$ for all the states in the (3, 3) manifold it is not given explicitly in the designation. For each M-component, the maximum intensity has been normalized to unity. In general, the $M = 0$ components have maximum intensity at $\theta = 0°$ (and $\theta = 180°$), and the component which has the largest M for each L has the maximum intensity at $\theta = 90°$. Components with intermediate values of M have maximum intensity occur at angles between 0° and 90°. Exceptions occur for the three $^1S^e$ states which have isotropic angular distributions and for the (1, 1) $^1D^o$ state. For the latter the maximum intensity for the $M = 1$ component occurs at 0° and the $M =$ component has zero intensity at this angle. The (1, 1) $^1D^o$ state differs from the rest in the (3, 3) manifold in that its parity and angular momentum is related by $\pi = (-1)^{L+1}$ while for all the others, $\pi = (-1)^L$. Another exception occurs for the (1, 1) $^1P^o$ state which appears to be almost isotropic for each of the $M = 0$ and the $M = 1$ components. The reason for this 'flatness' does not come from the angular factors, but rather from the interplay of the partial widths to $2s\varepsilon p$, $2p\varepsilon s$ and $2p\varepsilon d$ channels and the Coulomb phase of each channel. We checked the angular distributions for this state along the isoelectronic sequence and found that it becomes flatter with increasing Z.

3.2. Auger electron energy spectra for the (2, 3) doubly excited states of C^{4+} from double capture in C^{6+}–He collisions

The discussion in (3.1) neglects the width of each doubly excited state. When the width of a state is comparable to the separation between neighbouring states, a coherent sum of the electron emission amplitudes from different states is needed. The energy dependence of the electrons is also affected by the post-collision interaction. Both effects

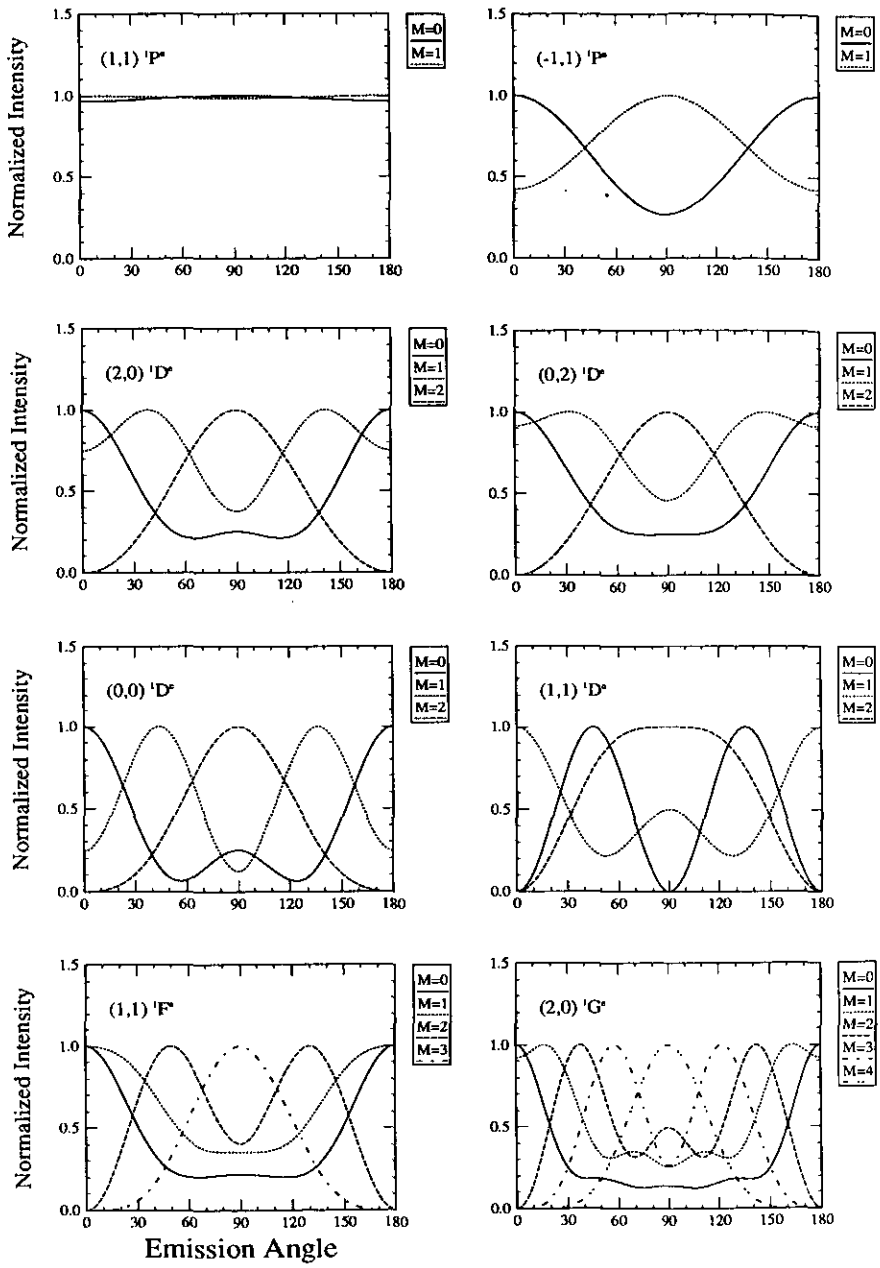

Figure 1. The angular distribution of Auger electrons from the autoionization of an isolated $3l3l'$ doubly excited state of O^{6+}. The dependence on the quantum number M for each state is shown with the maximum intensity for each component normalized to unity. Each state is labelled by the quantum numbers $(K, T)^{+\,1}L^{e,o}$.

are included in equation (6). From the calculated amplitudes for the formation of doubly excited states and the Auger decay amplitudes, the electron spectra at each electron's ejection angle can be calculated. Recall that the lineshape function reduces to Lorentzian in the absence of the PCI effect. The angular dependence of the electron spectra is determined primarily from the $Y_{l_2m_2}(\boldsymbol{k})$ term of each decay channel, but the shape function $f^{\alpha}(\varepsilon, \varepsilon_L)$ also has a weak angular dependence.

The atomic parameters for each of the ten states in the (2, 3) manifold are given in table 1. Each state is numbered from 1 to 10 according to the increasing Auger electron energies and each is designated using the $(K, T)^A$ quantum numbers (Lin 1986) besides L, S and π. Since $n=3$ and $N=2$ for all these states, these principal quantum numbers are not listed. In table 1 we also list the experimental Auger electron energies from Sakaue *et al* (1990). (In this reference one can find the comparison with theoretically calculated energies.) The total Auger rates, the radiative rates, and the branching ratio for Auger decays are calculated by us using the configuration-interaction method (Chen and Lin 1989). In table 1 we also list the Auger rates for $^1S^e$ and $^1P^o$ states calculated by Ho (1981). The Auger and radiative rates for this manifold have been calculated also by Stolterfoht *et al* (1990). Our results differ from theirs. It is noted that these states decay primarily by the Auger process, but there are two states, $(1,0)^-\ ^1P^o$ and $(-1,0)^0\ ^1P^o$, which have radiative rates comparable to Auger rates. In table 1 we also tabulate the total double capture cross section to each doubly excited state in the (2, 3) manifold for the C^{6+}-He collision at 67 keV calculated from the preceding paper (Chen *et al* 1991).

Table 1. Auger energies, Auger (R_a) and radiative (R_r) rates, Auger yields (ω_a) and double capture cross sections to individual doubly excited states in the (2, 3) manifold of C^{4+} for 67 keV C^{6+}-He collisions.

No	Label	E (eV)	R_a (10^{12} s^{-1})	R_r (10^{12} s^{-1})	ω_a	σ (10^{-17} cm^2)
1	$(1,0)^-\ ^1P^o$	323.7[a]	0.40[b] (0.34[c])	0.50[b]	0.44[b]	0.928[d]
2	$(1,0)^+\ ^1S^e$	324.7	167.54 (135.20)	0.24	1.00	0.680
3	$(0,1)^-\ ^1P^e$	325.5		—		0.512
4	$(0,1)^-\ ^1D^o$	327.0		—		0.526
5	$(1,0)^+\ ^1D^e$	327.5	96.13	0.64	0.99	1.093
6	$(0,1)^+\ ^1P^o$	328.7	68.46 (53.90)	0.55	0.99	1.184
7	$(0,1)^0\ ^1D^e$	329.9	37.38	0.36	0.99	1.325
8	$(1,0)^0\ ^1F^o$	330.2	12.21	0.82	0.94	0.969
9	$(-1,0)^0\ ^1P^o$	331.2	0.97 (1.32)	1.59	0.38	0.604
10	$(-1,0)^+\ ^1S^e$	332.6	6.24 (4.12)	0.67	0.90	0.257

[a] Experimental Auger electron energies from Sakaue *et al* (1990).
[b] From the present CI calculations.
[c] From Ho (1981).
[d] From the present coupled-channel calculations.

In figure 2 the electron energy spectra resulting from the Auger decay of double capture to C^{4+} ($2l3l'$) states in C^{6+} collisions with He at 67 keV are shown for the electron ejection angle of $\theta=0°$. In figure 2(a), the spectra are obtained by treating each state independently and neglecting the PCI effect. In this approximation, each resonance has a Lorentzian shape and the width of each state reflects the Auger width of that state. (The width of each state is given in table 1.) In figure 2(b) the effect of PCI is included and the contribution to the electron spectra from each state is treated

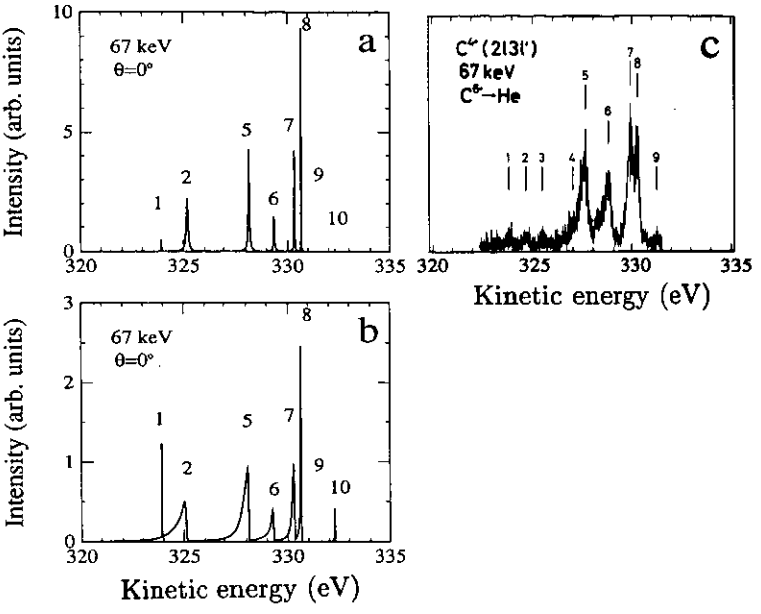

Figure 2. Electron spectra at 0° for the $2l3l'$ manifold of C^{4+} resulting from the collision of bare carbon ions with helium atoms at 67 keV. (*a*) Theoretical spectra assuming that each state decays incoherently and no PCI effect is included. For narrow lines, the actual width may be smaller than what was shown. (*b*) Theoretical spectra including the PCI effect and that the Auger decay from all the states has been treated coherently. (*c*) The experimental electron spectra from Sakuae *et al* (1989, 1990).

coherently. The scales in figure 2(*a*) and (*b*) are identical. It is clear that the PCI effect broadens and shifts the strength of each line toward lower energies. The atomic parameters for all the states in the (2, 3) manifold are listed in table 1, but in calculating the spectra using equation (6), the amplitudes for the formation and the Auger decay of each doubly excited state are used.

One can compare figure 2(*b*) with the experimentally determined electron spectra of Sakaue *et al* (figure 2(*c*)) measured at 0°. The overall agreement between figure 2(*b*) and experimental data is satisfactory. The theoretical spectra have not been convoluted with the electron energy resolution such that each line profile shows more pronounced skewness than the experimental one. The relative intensities among the lines also appear to be in qualitative agreement with the experiment. The Auger yield for each state has been included in the calculated spectra. Since the two states, $(0, 1)^-$ $^1P^e$ and $(0, 1)^-$, $^1D^e$, do not decay by electron emission, they are not seen in the theoretical electron spectra.

The electron energy spectra depend sensitively on the electron's ejection angle. To show this effect, the calculated spectra at $\theta = 60°$ and $\theta = 90°$ in the emitter frame are displayed in figures 3(*a*) and (*b*), respectively. Comparing them with figure 2(*b*) for the spectra at $\theta = 0°$, we note that the relative strength of individual states changes significantly with the electron's ejection angles. One cannot assume that the relative double capture cross sections to individual states are isotropic. When the PCI effect and the interference between neighbouring states can be neglected (experimentally this means that the spectral line is symmetric for each state and the angular distribution is symmetric with respect to $\theta = 90°$ in the emitter frame), the cross sections to individual

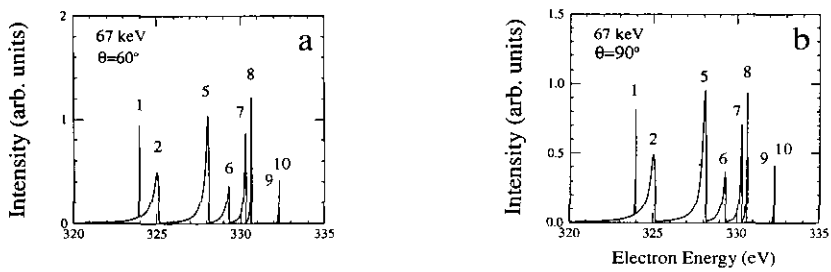

Figure 3. Electron spectra at (*a*) 60° and (*b*) 90° for the 2*l*3*l*′ manifold of C^{4+} resulting from the collision of bare carbon ions with helium atoms at 67 keV calculated by treating the decay from all the states coherently and including the PCI effect.

states can be extracted by measuring the electron spectra at a few angles. Recall that in this case the angular distribution of each state is given by equation (5) where the A_l parameters can be determined from the experiment. Such measurements have been carried out by Holt *et al* (1991) for double capture to 1s2*l*2*l*′ states in C^{5+} + He collisions recently.

3.3. Auger electron energy spectra for the (3, 3) doubly excited states of O^{6+} from double capture in O^{8+}–He collisions

The analysis of Auger electron energy spectra for the (3, 3) doubly excited states of O^{6+} resulting from the double capture in slow O^{8+}–He collisions is more complicated. There are three important differences for this system as compared to the (2, 3) states discussed above. First, each state can decay to 2*s* and 2*p* states of the O^{7+} ion. Second, the emitted Auger electrons have smaller energies; they are in the range of 34–50 eV. Third, the Auger widths of a number of states are comparable to the energy separations between neighbouring states.

The atomic parameters for the eleven singlet states within the (3, 3) manifold are shown in table 2. For convenience, we number each state starting with the lowest one, but each state is also labelled by the K and T quantum numbers. Since $A = +1$ for all the states in the manifold, this quantum number was not given explicitly. In table 2 we show the theoretical energies calculated by Ho (quoted in Mack *et al* (1989)). (The experimental energies quoted in Mack *et al* (1989) have been found to be in error (Morgenstern 1991).) The Auger width and the double capture cross section to each state (for 96 keV O^{8+} ions on He) from our calculation are also shown. The branching ratios for Auger decay to 2s and 2p states were obtained from the calculations by Bachau as quoted in Chetioui *et al* (1989). In calculating the electron spectra, we used the energies and widths from Ho in the PCI model but the Auger decay amplitudes needed in the calculation of the spectra are from our own CI calculations. Our calculated energies and widths do not differ significantly from Ho's.

We first illustrate the angular distribution if each doubly excited state in the (3, 3) manifold is treated independently and if the PCI effect is not included. The calculated electron spectra are shown in figure 4(*a*) at $\theta = 60°$ where each state displays a Lorentzian lineshape. When the width is large compared with the energy separation with the neighbouring states, the two lines overlap and the electron spectra appear to

Table 2. Parameters for the eleven states in the (3, 3) manifold of O^{6+}: Auger energies (E), Auger width (Γ_a), ratio of partial widths, $\Gamma(2s)/\Gamma(2p)$ for the Auger decay to 2s and 2p states, and capture cross sections to individual doubly excited states in the (3, 3) manifold of O^{6+} for 96 keV O^{8+}–He collisions.

No	(K, T)	E (eV)	Γ_a (eV)	$\Gamma(2s)/\Gamma(2p)$	σ (10^{-16} cm^2)
1	$(2, 0)\ ^1S^e$	34.68[a]	0.138[a]	0.12[b]	0.158[c]
2	$(2, 0)\ ^1D^e$	36.15	0.176	0.15	0.866
3	$(1, 1)\ ^1P^o$	37.40	0.381	0.49	0.771
4	$(1, 1)\ ^1D^o$	37.94	0.0084	0.00	0.262
5	$(0, 2)\ ^1D^e$	40.01	0.329	0.92	0.421
6	$(0, 0)\ ^1S^e$	40.36	0.569	0.17	0.094
7	$(2, 0)\ ^1G^e$	42.41	0.708	0.18	0.359
8	$(1, 1)\ ^1F^o$	42.82	0.362	0.24	1.604
9	$(0, 0)\ ^1D^e$	45.09	0.114	0.35	0.382
10	$(-1, 1)\ ^1P^o$	46.46	0.118	0.03	0.336
11	$(-2, 0)\ ^1S^e$	50.64	0.069	1.70	0.063

[a] Theoretical results from Ho as quoted in Mack *et al* (1989).
[b] From Chetioui *et al* (1989).
[c] From the present coupled-channel calculation.

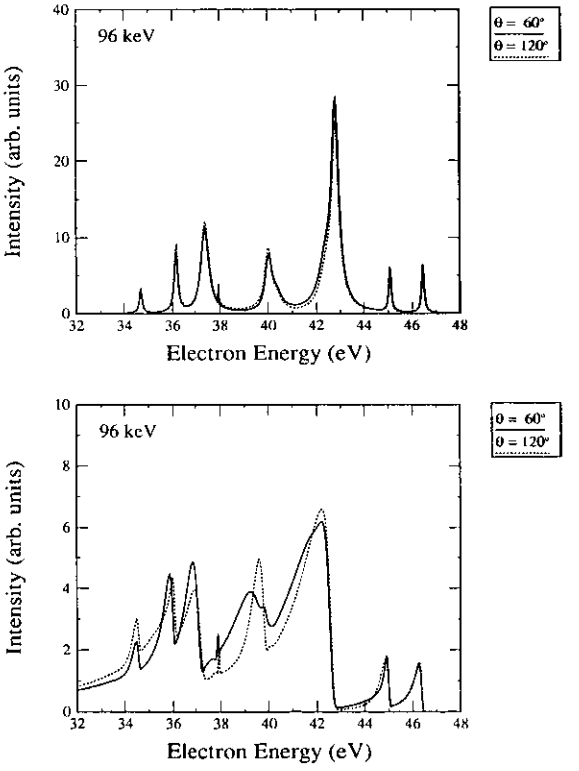

Figure 4. Electron spectra at 60° and 120° from the decay of (3, 3) states of O^{6+} formed in double capture in O^{8+}–He collisions at 96 keV. (*a*) Each state is treated independently and no PCI effect is included. the results at the two angles are identical. (*b*) The PCI is included and all the states are treated coherently.

have asymmetric profiles. This occurs for the peak near 40 eV which consists of #5 and #6 states, and the peak near 43 eV which consists of #7 and #8 states. In this approximation, the electron spectrum is symmetric with respect to $\theta = 90°$.

The post-collision interaction effect is more important for slow Auger electrons. For each isolated state, the PCI effect shifts the intensity toward the low-energy side and broadens the apparent width of each state. It also has the effect of enhancing the overlap between neighbouring states. In figure 4(b) we show the electron spectra at $\theta = 60°$ calculated including the PCI effect and the coherence among the doubly excited states. It is clear that the electron distribution has been shifted to the lower energy region and that each 'line' has been broadened significantly. The PCI effect makes it practically impossible to identify the area under each peak with the electron's intensity associated with that state. The spectra are also no longer symmetric with respect to $\theta = 90°$ because of the interference among the states and the PCI effect. In figure 4(b) we also show the calculated electron spectra at $\theta = 120°$ which clearly is different from the spectra at $\theta = 60°$.

In their analysis of the electron spectra, Mack *et al* (1989) assumed that the intensities from different doubly excited states can be treated as the incoherent sum from individual states (but including the PCI effect). We show in figure 5 the difference in the electron spectra at 60° when the amplitudes from different states are added up coherently (full curve) or incoherently (dotted curve). (The electron spectrum at 50° in the laboratory frame is approximately equal to 60° in the emitter frame for 96 keV O^{8+} on He). The discrepancy is not negligible. We next compare in figure 6 the theoretical electron spectra (from the full curves of figure 5) with the experimental data of Mack *et al* (1989). The agreement between the theoretical spectra and the experimental one is only qualitative. However, from a private communication (Morgenstern 1991), the experimental spectra had been found to be in error. In particular, the 'new' experimental energies are now in agreement with those calculated by Ho (see table 2). Since our spectra were calculated using Ho's energies, we expect that the locations of the peaks in figures 6(a) and (b) will be in agreement with the new data. Further comparison of experiment with this calculation has to wait until the new experimental spectrum becomes available. On the other hand, the 'pile-up' of

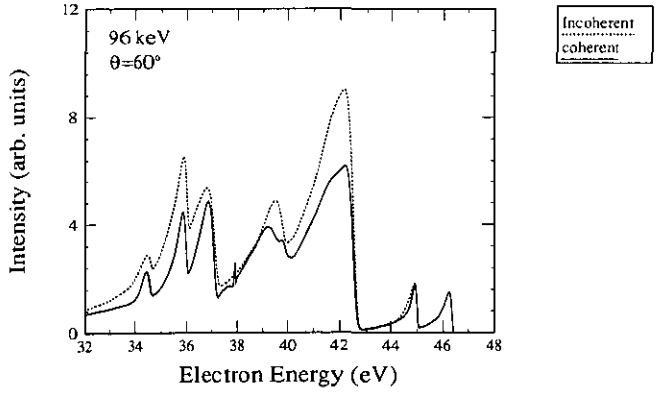

Figure 5. Theoretical electron spectra at 60° for the (3, 3) states of O^{6+}. The full curve is from treating electron emission from different states coherently, the dotted curve is from treating the emission incoherently. In both calculations the theoretical energies of Ho (1981) were used.

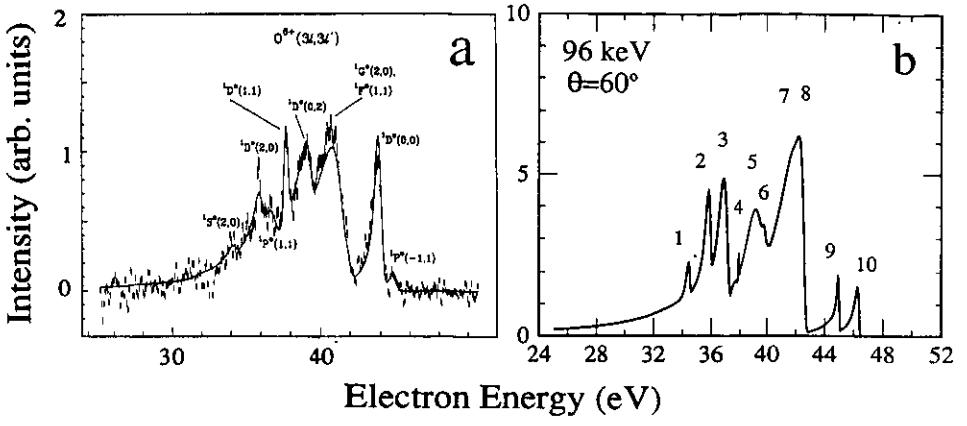

Figure 6. Comparison of the theoretical electron spectra at 60° in the emitter frame with the experimental electron spectra (see text).

electron intensity at lower energies is due to the PCI effect and is expected to remain the same.

Besides the independent-electron approximation used, we should mention that the present treatment of the PCI effect is incomplete. The present model treats the PCI effect of each state individually by multiplying the amplitude of each state by a shape function $f^{\alpha}(\varepsilon, \varepsilon_L)$. In the (3, 3) doubly excited states considered here, this treatment is inadequate. We note that states #7, #8 and #9 (see table 2), for example, are easily mixed by the electric field from the receding He^{2+} ions. In considering the PCI effect, these states should be treated together in a manner similar to the linear Stark effect as proposed in the literature (Stolterfoht *et al* 1979, Miraglia and Macek 1990).

The present calculation can also predict the electron spectra at any other angles. The zero-degree spectra for the (3, 3) doubly excited states of O^{6+} in O^{8+}-He collisions have not been measured yet. In view of the wide usage of zero-degree Auger spectrometers in many laboratories we show in figure 7 our predictions of the electron spectra for the collision energy of 96 keV which we hope can be tested in future experiments.

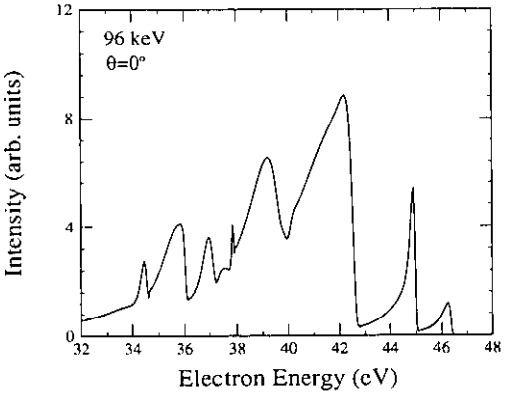

Figure 7. Theoretical electron spectra at 0° for the (3, 3) manifold of O^{6+} in O^{8+} collisions with He at 96 keV.

4. Summary and conclusions

In this paper we analyse the electron energy spectra of doubly excited states populated by double electron capture processes in slow collisions between multiply charged ions with atoms. In the theoretical calculations, we assume that doubly excited states are first populated by double capture, the ejected-electron spectra are obtained by following the electron emission from individual states. It is shown that one needs to include the post-collision interaction effect and that the emitted electrons from different states must be treated coherently. This is particularly true when the Auger electron energies are small and when the energy separations between neighbouring states are comparable or smaller than the widths of the states.

Doubly excited states populated in slow collisions are usually strongly aligned and the resulting ejected-electron spectra are not isotropic. We emphasize that it is extremely difficult to deduce double capture cross sections to individual doubly excited states by fitting the measured electron spectra at one angle only. Except for very special circumstances, the number of parameters to be fitted from the experimental data is too many and the fitted results may not be unique. When the PCI effect is large and/or when coherence is important, it is more desirable that the experimental electron spectra be compared with the theoretical electron spectra directly at different angles.

We have considered the electron energy distribution from the Auger decay of the (2, 3) doubly excited states of C^{4+}. These states decay to the 1s state of C^{5+} where the energies of the Auger electrons are of the order of 330 eV. In this case, the Auger decay of each doubly excited state can be treated independently and the PCI effect is negligible such that measurements of the electrons at a few angles would allow the determination of double capture cross sections to individual doubly excited states. We have also considered the Auger electrons from the (3, 3) states of O^{6+} following double capture in O^{8+}–He collisions. For this system the PCI effect is very large and the electron emissions from different states are all mixed such that the electron intensity under a peak cannot be attributed to individual states directly.

We have also shown that the calculated electron spectra for the (2, 3) manifold of C^{4+} are in good accord with the experimental data from the zero-degree Auger measurement. This is an indication that the independent-electron approximation used in the calculation of double capture cross sections is a reasonable model for the system considered. However, a more definite conclusion can be drawn only after comparing the calculaated electron spectra with those measured at other angles and at other energies. We did not have as much success for the electron spectra for the (3, 3) doubly excited states of O^{6+} from the O^{8+}–He collisions. However, the experimental results shown in Mack *et al* (1989) had now been found (Morgenstern 1991) to be in error. Comparison of our calculations has to wait until new experimental data become available.

Acknowledgment

This work is supported in part by the US Department of Energy, Office of Basic Energy Sciences, Division of Chemical Sciences. We thank R Morgenstern for much useful correspondence on the PCI effect. We also thank R Morgenstern and A Bordenave-Montesquieu for comments on the initial draft of the manuscript.

References

Aberg T and Howat G 1982 *Encyclopedia of Physics* ed S Flugge and W Mehlhorn (Berlin: Springer) p 469

Arcuni P W 1986 *Phys. Rev.* A **33** 105

Barker R B and Berry H W 1966 *Phys. Rev.* **151** 14

Barrachina R O and Macek J H 1989 *J. Phys. B: At. Mol. Phys.* **20** 2151

Bordenave-Montesquieu A, Benoit-Cattin P, Boudjema M, Gleizes A, Dousson S and Hitz D 1988 *Proc. 15th Int. Conf. on the Physics of Electronic and Atomic Collisions (Brighton)* (Amsterdam: North-Holland) Invited papers p 551

Boudjema M, Cornille M, Dubau J, Moretto-Capelle P, Bordenave-Montesquieu A, Benoit-Cattin P and Gleizes A 1991 *J. Phys. B: At. Mol. Opt. Phys.* **24** 1713

Chen Z, Shingal R and Lin C D 1991 *J. Phys. B: At. Mol. Opt. Phys.* **24** 4215-30

Chen Z and Lin C D 1989 *J. Phys. B: At. Mol. Opt. Phys.* **22** 2875

Chetioui A, Bachau H, Wohrer K, Vernhet D, Blumenfeld L, Politis M F, Rozet J P, Touati A and Stephen C 1989 *J. Phys. B: At. Mol. Opt. Phys.* **22** 2865

Cleff B and Mehlhorn W 1974 *J. Phys. B: At. Mol. Phys.* 7 593

Devdariani A Z, Ostrovski V N and Sebyakin Yu N 1977 *Sov. Phys.-JETP* **46** 215

Ho Y K 1981 *Phys. Rev.* A **23** 2137

Holt R A, Prior M H, Randall K L, Hutton R, McDonald J and Schneider D 1991 *Phys. Rev.* A **43** 607

Lin C D 1986 *Adv. At. Mol. Phys.* **22** 76

Mack M, Nijland J H, van der Straten, Niehaus A and Morgenstern R 1989 *Phys. Rev.* A **39** 3846

Miraglia J and Macek J H 1990 *Phys. Rev.* A **43** 3971

Moretto-Capelle, Oza D H, Benoit-Cattin P, Bordenave-Montesquieu A, Boudjema M, Gleizes A, Dousson S and Hitz D 1989 *J. Phys. B: At. Mol. Opt. Phys.* **22** 271

Morgenstern R 1991 Private communication

Morgenstern R, Niehaus A and Thielmann U 1977 *J. Phys. B: At. Mol. Phys.* **10** 1039

Morgenstern R, van der Straten P and Niehaus A 1990 *Phys. Rev. Lett.* **64** 2589

Niehaus A 1977 *J. Phys. B: At. Mol. Phys.* **10** 1845

Posthumus J H and Morgenstern R 1990 *J. Phys. B: At. Mol. Opt. Phys.* **23** 2293

Sakaue H A 1990 *J. Phys. B: At. Mol. Opt. Phys.* **23** L401

Stolterfoht N, Brandt D and Prost M 1979 *Phys. Rev. Lett.* **43** 1654

Stolterfoht N, Sommer K, Swenson J K, Havener C C and Meyer F W 1990 *Phys. Rev.* A **42** 5396

van den Brink J P, van Eck J and Heideman H G M 1989 *J. Phys. B: At. Mol. Opt. Phys.* **22** 939

van der Straten P and Morgenstern R 1986a *Phys. Rev.* A **34** 4482

—— 1986b *J. Phys. B: At. Mol. Phys.* **19** 1361

van der Straten P, Morgenstern R and Niehaus A 1988 *Z Phys.* D **8** 35